Al-Nahrain Journal of Science
ANJS, Vol.25 (2), June, 2022, pp. 1-7

Green Synthesis of Magnesium Oxide (MgO NPs) and Adsorption with Eosin Dye

Alieaa H. Obaid[1], Fadhila M. Hussein[1], Salma A. Abbas[1], Asmaa A. Jawad[2,*] and Tahseen A. Ibrahim[3]

[1]Department of Chemistry, College of Science, University of Al-Mustansiriyah, Baghdad-Iraq
[2]Forensic DNA Research and Training Center, Al-Nahrain University, Baghdad-Iraq
[3]Ministry of Health, Inspection Department, Baghdad-Iraq

Article's Information

Received: 26.03.2022
Accepted: 10.05.2022
Published: 30.06.2022

Keywords:
Magnesium Oxide (MgO) nanoparticles
Adsorption
Eosin dye
Green synthesis

DOI: 10.22401/ANJS.25.2.01

*Corresponding author: asmaa85ali@gmail.com

Abstract

The green synthesis method is used to create magnesium oxide (MgO) nanoparticles in this study. SEM measurements and X-ray diffraction techniques are used to determine their crystal structure, as well as, FTIR to analyze the MgO na articles. Green synthesis of MgO nanoparticles are a good adsorbent for Eosin dye in aqueous solutions. Contact time, adsorbent mass, temperature, and Eosin dye concentration were all investigated. Freundlich isotherm models and the Eosin dye isotherm adsorption were well identical. The thermodynamic research yielded 101.4152 J/mol K, 0.02826397 kJ/mol, and –30.7005537 kJ/mol for the ΔS, ΔH and ΔG parameters, respectively. moreover, with R^2 = 0.9228, the kinetic investigation revealed that the adsorption was pseudo-second-order.

1. Introduction

MgO s a widely used inorganic material [1]. It used in a variety of applications, including catalysis, catalyst supports, toxic waste treatment, resistance materials and adsorbents, Additive to heavy fuel oil, reflecting and anti-reflecting coating, As substrates, superconducting and ferroelectric thin films are used [2]. It is also used in medicine to treat dyspepsia, heartburn, Oncology treatment, and regenerate bone. MgO NPs are also used as an antibacterial [3].

Green synthesis of nanoparticles:

The green chemistry method that creates nanoparticles is environmentally friendly [4]. Lately the plant extract is considered non-toxic, not in the materials from which it is produced. Also when it is produced, and is completely safe [5]. The method used to produce the extract is a simple, uncomplicated, and inexpensive method [6] Phenolic acids, bioactive polyphenols, sugars, proteins, alkaloids, and terpenoids are all found in plant extracts [7].

Types of adsorption:

Physical adsorption: The forces that cause occurrence of physical adsorption (abbreviated Physisorption) are related to the same kind of forces that cause the formation of liquids which gets as a result of intensification of gases, which is usually called Vander Waals forces [8]. A rare-gas atom or a saturated molecule that is weakly attached to a surface is said to be in physical adsorption [9]. The heat of adsorption should be in the zone of heats of condensation (about 40 kJ. mol^{-1} or less), Physical adsorption achieves equilibrium quickly and by and large occur at low temperatures where it can be effectively reversible. Besides, this kind of adsorption is nonspecific and may expand to in excess of one layer of adsorbate on the adsorbent surface [10].

Chemical adsorption: Chemical adsorption (acronym for chemisorptions) occurs when molecules (or atoms) form a chemical bond (usually covalent) with the surface and then seek out sites with the highest number of coordinations with the substrate. Adsorption heat is significantly higher than physical adsorption heat (greater than about 80 kJ. mol^{-1}). Chemisorption is characterized by its specificity, which can be quick or slow. It is usually irreversible in nature and can happen at room temperature or higher temperatures [11]. To our knowledge, no systematic research has been done on the adsorption mechanisms of Eosin dye using MgO nanoparticles. To remove eosin dye from aqueous solutions, MgO nanoparticles made using the green synthesis approach were utilized. This experiment took into account the weight of the adsorbent, the contact time, the temperature, and the concentration of Eosin dye.

2. Experimental Setup

2.1 Materials:

Magnesium nitrate Hexahydrate ($Mg(NO_3)_2.6H_2O$), Plant Lemon Peel extract, NaOH, Sigma-Aldrich products were

purchased and used exactly as they were given to us (UK). Throughout the purification of the finished product, deionized water was employed.

2.2.1 Preparation of lemon peel extract:

Powder was produced from Lemon peel by collecting Lemon peels, washing it to remove all impurities and the peels were dried and grinded until they turn into powder. 10 gm of powder was dissolved in 100 ml of deionized water and it has been refluxed for 1 hr. Then extract was filtered using filter paper [12]

2.2.3 Preparation MgO NPs:

Plant Lemon Peel extract was added drop wise with stirring at room temperature to a solution of Magnesium Nitrate Hexahydrate (Mg $(NO_3)_2.6H_2O$) (0.1 M,400 ml) for (1.5) hrs. until The solution is cloudy (evidence of nanoparticle formation) then was added (0.05 M) of NaOH, then the precipitate is washed sundry times by deionized water for two days, at 120 °C, the sample was been dried in the oven for two hours, then calcination at (600 °C) for three hours,Adding the base to the nitrate solution contributes to the formation of magnesium hydroxide in the aqueous medium [13].

2.3 Characterization:

The MgO nanoparticles were analyzed using X-ray diffraction (XRD-6000), which was been operated at 40 kV and 30 mA to produce 1.5406 °A wavelength radiation. JEM-2100 JEOL (Japan), AFM photos of (MgO) nanoparticles and their size distributions, AFM is employed in morphological research because it generates topological images of surfaces at extremely high enlargement, making it easy to view the atomic structure of crystals. The diameters of MgO nanoparticles were determined using scanning electron microscopy (SEM). The spectrum of MgO nanoparticle was demonstrated using Fourier-transform infrared spectrophotometer (FTIR) Shimadzu 4800S (USA).

2.4 Adsorption of eosin dye on MgO:

500 ml of 30 ppm stock eosin dye prepared by weighting 0.015 gm of eosin dye and it was prepared different concentrations between (5-25 ppm) from the stock solution Eosin dye, MgO nanoparticles (0.007 gm) were had been added to various solutions and shackled for 80 minutes at various temperatures: 15 °C, 30 °C, 45 °C, and 60 °C. These solutions were had been filtered and passed through a UV-VIS spectrophotometer to quantify the concentration of Eosin dye, used the equation below [14,15]:

$$Qe = (C_0 - C_e)\, V\text{sol.} / M \quad \ldots(1)$$

where Qe is the equilibrium adsorption capacity(mg/g), C_e and C_0 are the equilibrium and initial Eosin dye concentrations (mg/L), Vsol. is the liquid volume (L), and M is the weight of the MgO nanoparticle (g).

3. Results and Discussion

3.1 Characterization of MgO nanoparticle:

To determine the nature of the powders produced, all samples were subjected to XRD analysis; appeared the XRD peaks of the MgO crystal-style structure at angles ranging from 30° to 80°. According to the standard MgO nanoparticle patterns, the high peaks at 31.82°, 34.79°, 36.43°, 47.73°, 56.36°, 63.25°, 68.41° and 77.18° which are corresponding to 100, 002, 101, 102, 110, 103, 112 and 004 Muller values, respectively, as show in the Figure 1. The FTIR spectra of MgO nanoparticles is illustrated in the Figure 2. At 466 cm^{-1} due to the bending vibration of Mg–O, this correspond with the results of Balakrishnan G. et al. [16], who claimed that the wide band at 473 cm^{-1} referred to Mg–O bending vibrations [16],The peaks observed in the range 450 to 560 cm^{-1} are specific to Mg–O vibrations[17]. Other researchers confirmed that the peaks at 427 to 619 cm^{-1} observed in the FTIR spectrum are due to Mg-O vibration[18]. The peak at 3515 cm^{-1}, indicates the O–H group's stretching vibration [19]. The peak at 1474.46 cm^{-1} and 1354.84 cm^{-1} indicating the C–H bending of alkanes [19]. SEM was used to evaluate the shape and size of the main nanoparticle, illustrated in the Figure 4.

3.2 Adsorption isotherms:

Fitting isotherm adsorption with adsorption results to identify how adsorbent Eosin dye works was the most crucial stage of the adsorption investigation. the isotherms of Freundlich and Langmuir were investigated in this paper. The correlation factor R^2 demonstrates that Freundlich isotherm equations fit the adsorption results very well, as shown in Figure 5. The equation below is the linearized form of Freundlich isotherms [20,21]:

$$\ln qe = \ln K_{Fr} + (1/nf)\ln Ce \quad \ldots(2)$$

where the indices of adsorption capacity and intensity, kf and n, are also known as the Freundlich constants. The intercept is used to determine the K_{Fr}, while the slope is used to calculate the n, demonstrated in Figure 5(a). This project calculated the Freundlich isotherm for MgO as (1/n), which was 1.4128. This result was consistent with the favorable physical adsorption. [22]. The data, however, did not fit the Langmuir adsorption isotherm, as indicated in the equation below [23].

$$Ce / qe = 1 / q_{\max} K_L + Ce / q_{\max} \quad \ldots(3)$$

where qe is the amount of dye adsorbed at equilibrium (mg/g), Ce is the adsorbate concentration at equilibrium (mg/L), K_L is the Langmuir isotherm constant (L/mg), and q_{max} is the maximal monolayer coverage capacity (mg/g). The rate of adsorption was relent less from the linear equation of specific adsorption Ce⁄Qe vs. Ce. demonstrated in Figure 5(b).

$$R_L = 1/ (1 + K_L C_i) \quad \ldots(4)$$

where C_i: represents is the concentration initial of Eosin dye(mg/L), the R_L values are all between 0 and 1, showing that Eosin dye adsorption on MgO nanoparticles is preferred.

3.3 Influence of contact time:

The influence of contact time was investigated at 303K with 10 mg/L Eosin dye and 0.007 g MgO nanoparticle from (10 -110) minutes. However, Figure 6 shows that the amount of adsorption increases directly with the raise in dye concentration, with eosin adsorption occurring rapidly from the start of the trials until 80 minutes. This could be owing to the nanoparticles' surface having unoccupied adsorption sites, which increase until the time exceeds 80 to attain equilibrium [24].

3.4 Effect of dye concentrations:

Concentration effect of eosin dye on MgO nanoparticles was experimentally studied under the following conditions: the dye concentration range are (5, 10, 15, 20 and 25) mg/L, and the mass of nanoparticles is (0.006) g, at 303 K, the stirring time is 80 minutes. It can be observed from Figure 7. It may be assumed that as the initial dye concentration rises from 5 to 25 mg/L, the initial Eosin concentration rises, resulting in an increase in adsorption [24].

3.5 The weight MgO nanoparticles:

The effect quantity adsorbent material on the dye removal rate by MgO nanoparticles as an adsorbent was performed using various nanoparticles weight (0.004, 0.006, 0.008,0.01 and 0.012 g) at 10 mg/L dye at 303 K, the stirring time is 80 minutes, As shown in Figure 8, the adsorption rate is speedy due to the increased active site of MgO nanoparticles and increased adsorption of dye was shown by increasing the amount of adsorbent [24].

3.6 Temperature effect and thermodynamic parameter calculation:

At temperatures of 288, 303, 318, and 333 k, the temperature impact of Eosin dye adsorption on MgO nanoparticles' surfaces was investigated. With increasing temperature, the amount of dye adsorption solution increased shown in Figure 9. This indicates that the process was endothermic, with a positive mean of ΔH. This is evidence of the occurrence of the process of adsorption as well as absorption [20]. Moreover, as the temperature raise. The molecules of diffusion were absorbed by the pores, rising spread rates also the potent relation between the adsorbent and the adsorbate. The parameters of thermodynamics give precise information on the intrinsic energy changes associated with adsorption. The following variations were had been estimated to foretell the adsorption operation Utilization the adsorption free energy (ΔG), enthalpy (ΔH), and entropy (ΔS) based on the following equations [20, 25-28]:

$$\mathrm{Ln}Keq = -\Delta H/RT + \Delta S/R \quad \ldots(5)$$

$$Keq = qe / Ce \quad \ldots(6)$$

$$\Delta G = \Delta H - T\,\Delta S \quad \ldots(7)$$

where; T is the absolute temperature (K), Keq is the ability of adsorbate to retain and a measure of its movement within the solution, R is the general of gases constant (8.314 $J.K^{-1}mol^{-1}$), qe (mg/gm) is the equilibrium capacity of adsorption, The slope and intercept of the linear Vants Hoff plot of lnKeq vs. $1/T$, can be used to calculate the values of ΔH and ΔS, respectively, show in Figure 10. The slope's congruous ΔH was (0.02826397 kJ/mol), Indicates that the endothermic process. The ΔS value from the intercept was (101.4152 J / (mol.K)), shown that the molecules that have been adsorbed as yet moving on the surface. The adsorption of eosin dye was aided by a higher temperature. The adsorption ΔG was calculated to be (−30.7005537 kJ/mol), indicating that adsorption occurred spontaneously.

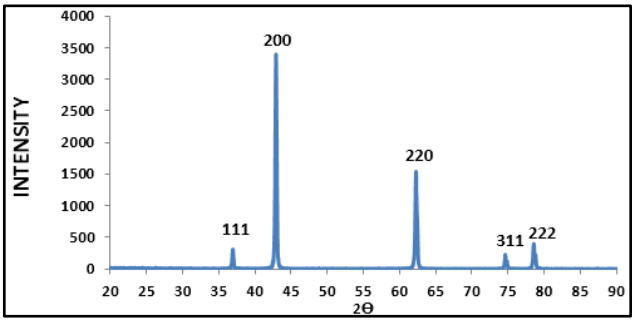

Figure 1. The diffraction peaks MgO NPs by using XRD were identified by comparison with pattern of standard (MgO) (37.37°, 43.14°, 62.25°, 74.94° and 78.85°) these peaks correspond the reflection planes (111), (200), (220), (311) and (222) respectively. Through the resulting peaks, it indicates that the structure is cubic for MgO.

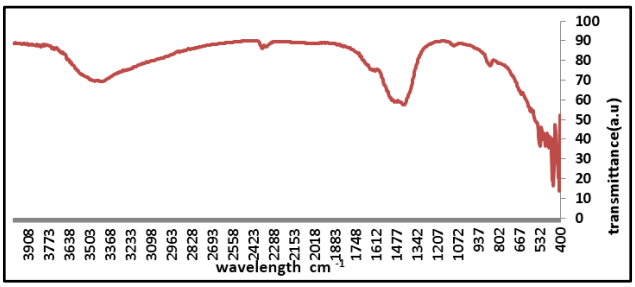

Figure 2. The spectrum of FTIR several peaks is shown, namely: the band is observed at 466 cm^{-1} due to the bending vibration of Mg-O, the peak at 3515 cm^{-1} represents the stretching vibration of the OH group, the peak at 1474.46 cm^{-1} and 1354.84 cm^{-1} indicates the bending C–H for alkanes.

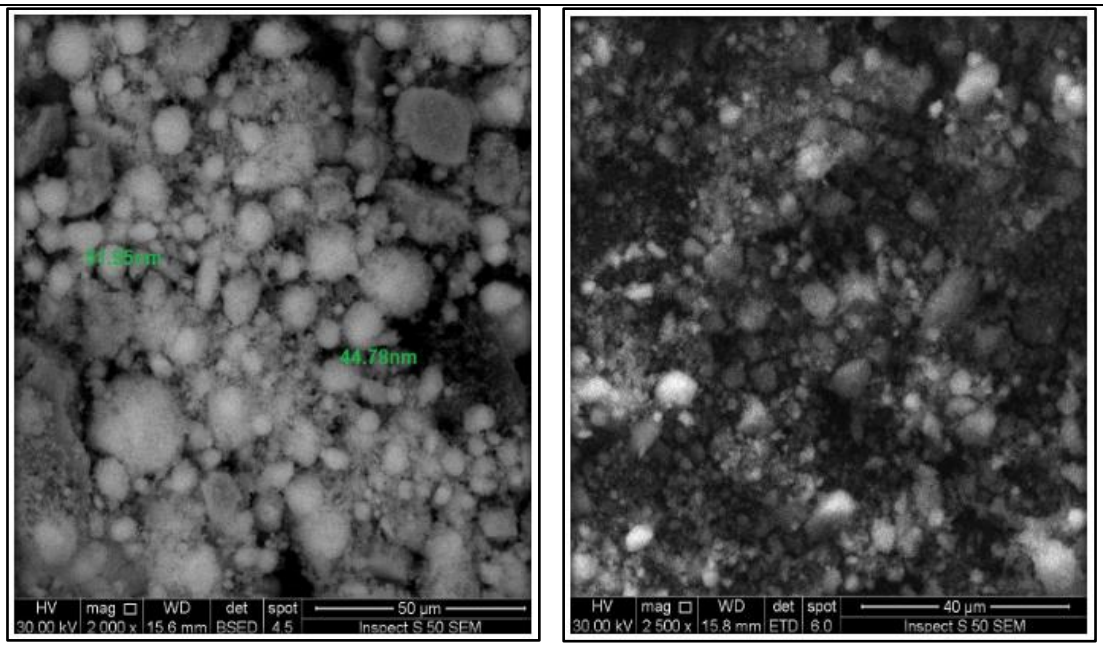

Figure 3. SEM Micrographs of the MgO nanoparticles. Demonstrates arrangement within the crystal structure.

Avg. Diameter: 41.04 nm, 10% Diameter: 19.00 nm, 50% Diameter: 32.00 nm, 90% Diameter: 63.00 nm

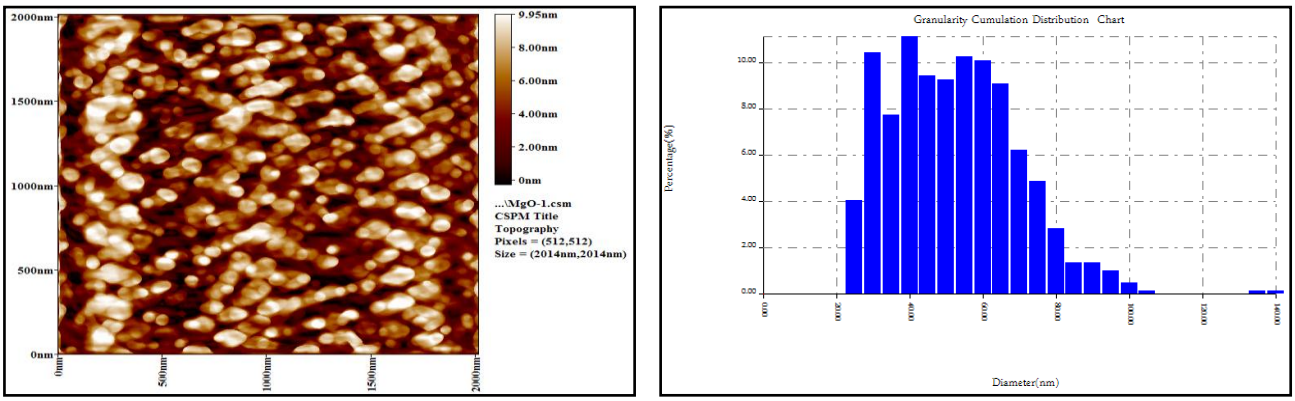

Figure 4. Shows the dimensions of AFM images the Versus size distribution of (MgO NPs). AFM is used for morphological analysis because it produces topological images of surfaces at a very high enlargement and makes it easier to see the crystals's atomic structure, where the results indicated that the particle MgO average diameter (41.04 nm).

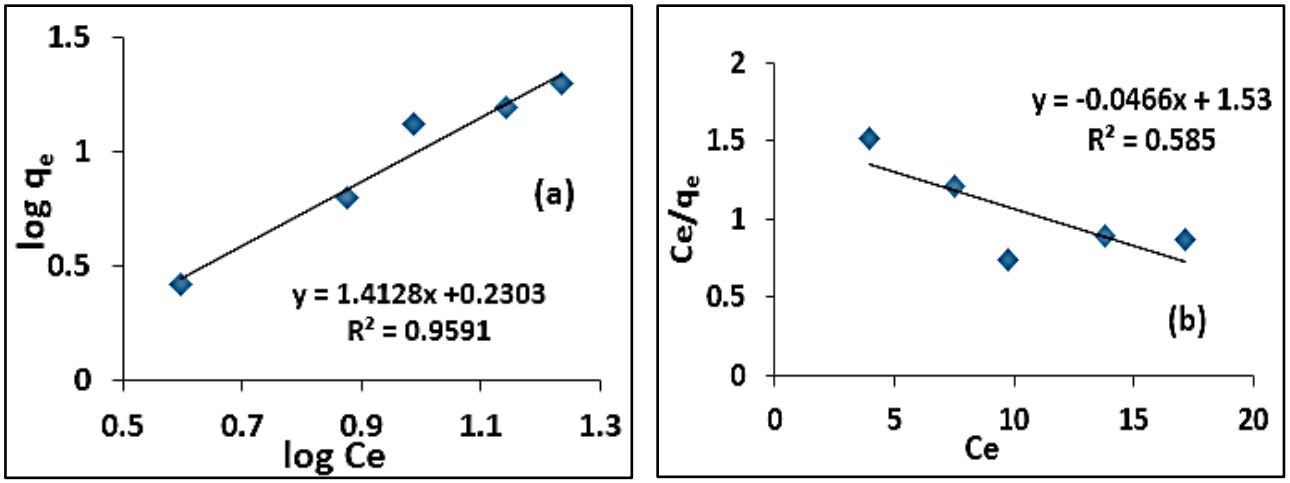

Figure 5. Adsorption curves of (a) Freundlich isotherm and (b) Langmuir isotherm at 303 K. We notice the correlation factor R^2 demonstrates that Freundlich isotherm equations fit the adsorption results very well.

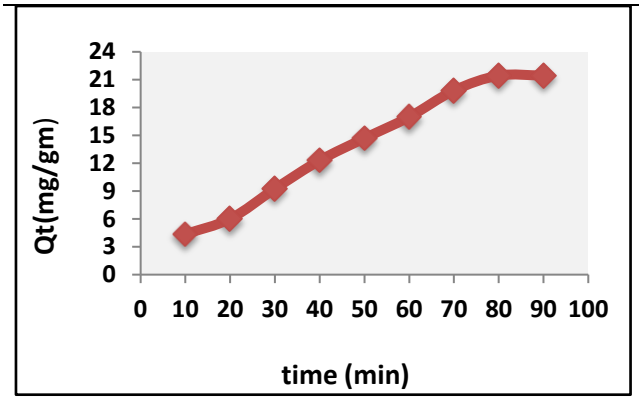

Figure 6. The influence of contact time. We notice that the equilibrium time is 80, which is the time after which no decrease in Eosin concentration.

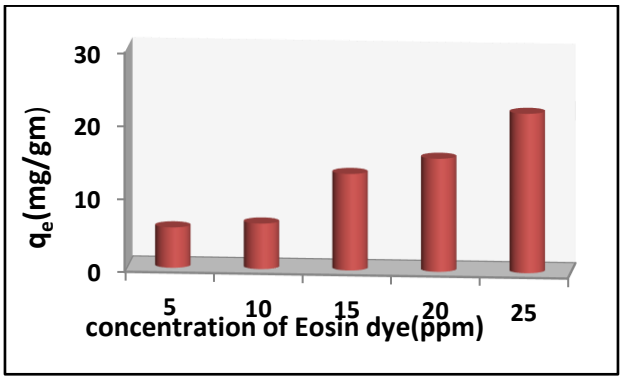

Figure 7. Shows increase in the adsorption capacity with increasing concentration Eosin dye.

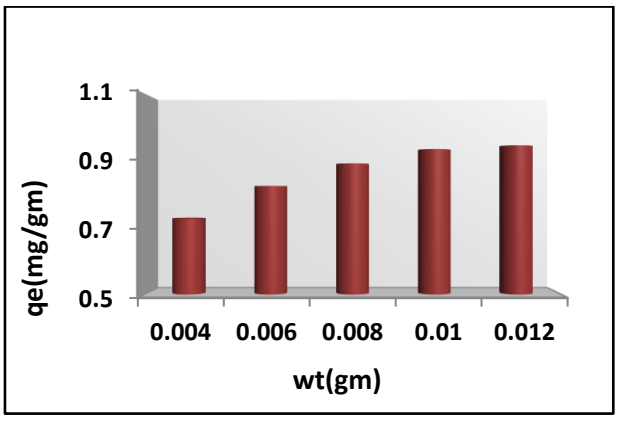

Figure 8. Shows increase in the adsorption capacity with increasing weight of MgO NPs.

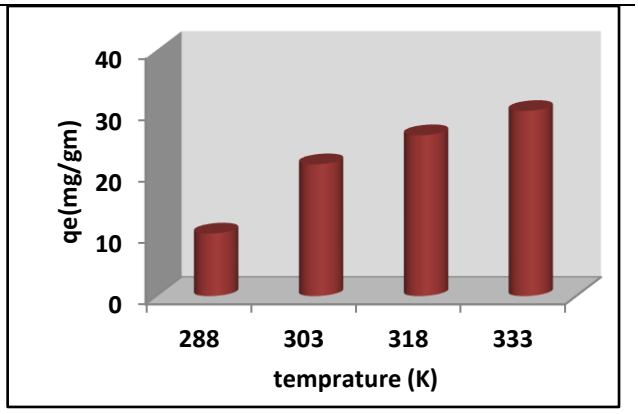

Figure 9. Shows increase in the adsorption capacity with increasing temperature.

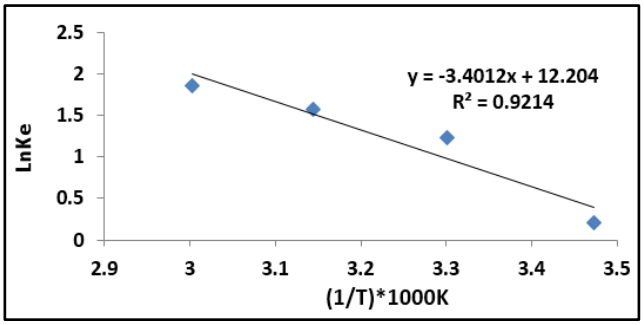

Figure 10. Van't Hoff plots of the dye adsorption at different temperatures. To know the values of thermodynamic functions (ΔH, ΔS, and ΔG).

3.7 Dynamics:

The adsorption kinetics of Eosin dye on the surface. The adsorbents of MgO nanopartcales are critical in adsorbent applications. The adsorption equilibrium time for 0.007 g of MgO NPs adsorbents was found to be around 80 min in the research of Eosin dye. Moreover, the following kinetic models and classical were utilized in this work to characterize the adsorption information described above: Pseudo-first-order model by the equation (8) [22,29,30]:

$$\ln (qe - q_t) = \ln qe - k_1 t \quad \ldots(8)$$

The equation represents a pseudo-second order kinetic model (9) [20,31].

$$t/q_t = 1 / k_2\, qe^{\,2} + (1/qe)t \quad \ldots(9)$$

where qe and qt are the equilibrium and time adsorbent Eosin dye concentrations (mg/g), respectively, and k_1 and k_2 they are the kinetic rate constants. A pseudo-second-order model with a high correlation coefficient ($R^2 > 0.9228$) may accurately capture the kinetic information (Figure 11).

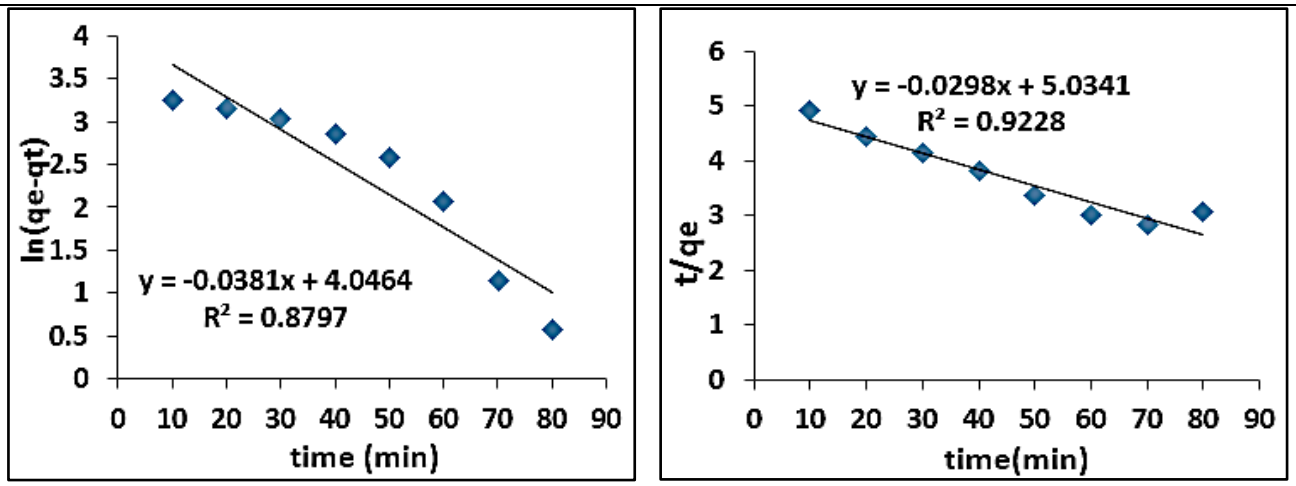

Figure 11. Dynamic of adsorption of Eosin dye: (a) pseudo-first-order and (b) pseudo-second-order. Through the value of the correlation coefficient ($R^2 > 0.9228$), it is Appear that the reaction kinetics is of the pseudo-second order.

4. Conclusion

According to XRD, SEM, and FTIR characterizations, the green synthesis approach produced good quality MgO NPs. All techniques gave information indicating that the product is MgO was nanoparticl, with an average crystal size of 41.78 nm. For removing Eosin dye from aqueous solutions, the MgO nanoparticle Has proved to have good adsorption characteristics of eosin dye. The efficacy of MgO nanoparticle adsorption has been demonstrated in both dynamic and kinetic investigations. Freundlich isotherm models were found to be well suited to the data. The adsorption values for ΔH, ΔS, and ΔG were calculated to be 0.02826397 kJ/mol, 101.4152 J/mol K, and −30.7005537 kJ/mol, respectively, based on the thermodynamic characteristics these findings show that adsorption is a spontaneous endothermic process that exhibits pseudo-second-order behavior with $R^2 = 0.9228$.

Conflicts of Interest

The authors declare that there is no conflict of interest.

References

[1] Al-Gaashani R.; Radiman S.; Al-Douri Y.; Tabet N. and Daud A. R.; "Investigation of the optical properties of Mg (OH) 2 and MgO nanostructures obtained by microwave-assisted methods", J. Alloys Compd.; 521: 71-76, 2012.

[2] Ouraipryvan P.; Sreethawong T. and Chavadej S.; "Synthesis of crystalline MgO nanoparticle with mesoporous-assembled structure via a surfactant-modified sol-gel process", Mater. Lett.; 63(21): 1862-1865, 2009.

[3] Mirzaei H. and Davoodnia A.; "Microwave assisted sol-gel synthesis of MgO nanoparticles and their catalytic activity in the synthesis of hantzsch 1, 4-dihydropyridines", Chinese J. Catal.; 33 (9-10): 1502-1507, 2012.

[4] Nayak S.; Sajankila S. P.; Rao C. V.; Hegde A. R. and Mutalik S.; "Biogenic synthesis of silver nanoparticles using Jatropha curcas seed cake extract and characterization: evaluation of its antibacterial activity", Energy Sources, Part A Recover. Util. Environ. Eff.: 1-9, 2019.

[5] Castro L.; Blázquez M. L.; Muñoz J. A.; González F.; García-Balboa C. and Ballester A.; "Biosynthesis of gold nanowires using sugar beet pulp", Process Biochem.; 46 (5): 1076-1082, 2011.

[6] Asmathunisha N. and Kathiresan K.; "A review on biosynthesis of nanoparticles by marine organisms", Colloids Surfaces B Biointerfaces, 103: 283-287, 2013.

[7] Premanathan M.; Karthikeyan K.; Jeyasubramanian K. and Manivannan G.; "Selective toxicity of ZnO nanoparticles toward Gram-positive bacteria and cancer cells by apoptosis through lipid peroxidation", Nanomedicine Nanotechnology, Biol. Med.; 7 (2): 184-192, 2011.

[8] Somorjai G. A. and Li Y.; "Introduction to surface chemistry and catalysis", John Wiley & Sons, 2010.

[9] Atkin R.; Craig V. S. J.; Wanless E. J. and Biggs S.; "Mechanism of cationic surfactant adsorption at the solid–aqueous interface", Adv. Colloid Interface Sci.; 103 (3): 219-304, 2003.

[10] Atkins P. and De Paula J.; "Elements of physical chemistry", Oxford University Press, USA, 2013.

[11] Perego C. and Peratello S.; "Experimental methods in catalytic kinetics", Catal. Today, 52 (2-3): 133-145, 1999.

Abdallah Y.; Ogunyemi S. O.; Abdelazez A.; Zhang M.; Hong X.; Ibrahim E. and Chen J.; "The green synthesis of MgO nano-flowers using Rosmarinus officinalis L. (Rosemary) and the antibacterial activities against Xanthomonas oryzae pv. oryzae". BioMed Research International, 2019, 2019.

[13] Bhattacharya P.; Swain S.; Giri L. and Neogi S.; "Fabrication of magnesium oxide nanoparticles by solvent alteration and their bactericidal applications", J. Mater. Chem. B, 7 (26): 4141-4152, 2019.

[14] Svecova L.; Dossot M.; Cremel S.; Simonnot M. O.;

Sardin M.; Humbert B. and Michot L. J.; "Sorption of selenium oxyanions on TiO_2 (rutile) studied by batch or column experiments and spectroscopic methods", Journal of hazardous materials, 189 (3): 764-772, 2011.

[15] Mohammed M. A.; Rheima A. M.; Jaber S. H. and Hameed S. A.; "The removal of zinc ions from their aqueous solutions by Cr_2O_3 nanoparticles synthesized via the UV-irradiation method", Egypt. J. Chem., 63(2): 425-431, 2020.

[16] Balakrishnan G.; Velavan R.; Batoo K. M. and Raslan E. H.; "Microstructure, optical and photocatalytic properties of MgO nanoparticles", Results Phys., 16: 103013, 2020.

[17] Vergheese M. and Vishal S. K.; "Green synthesis of magnesium oxide nanoparticles using Trigonella foenum-graecum leaf extract and its antibacterial activity", J Pharmacogn Phytochem, 7 (3): 1193-1200, 2018.

[18] Kimbonguila A.; Matos L.; Petit J.; Scher J. and Nzikou J. M.; "Effect of physical treatment on the physicochemical, rheological and functional properties of yam meal of the cultivar 'Ngumvu' from Dioscorea alata L. of Congo", Int. J. Recent Sci. Res., 8: 22213-22217, 2019.

[19] Metelev I. and Marfin E.; "Changes in the properties of a porous medium by ultrasound exposure", In Tyumen, 2019, 2019 (1): 1-5, 2019.

[20] Hussain D. H.; Rheima A. M. and Jaber S. H.; "Cadmium ions pollution treatments in aqueous solution using electrochemically synthesized gamma aluminum oxide nanoparticles with DFT study", Egypt. J. Chem., 63 (2): 417-424, 2020.

[21] Rheima A. M.; Hussain D. H. and Almijbilee M. M. A.; "Graphene-silver nanocomposite: Synthesis, and adsorption study of cibacron blue dye from their aqueous solution", J. Southwest Jiaotong Univ., 54 (6), 2019.

[22] Rheima A. M.; Mohammed M. A.; Jaber S. H. and Hameed S. A.; "Adsorption of selenium (Se4+) ions pollution by pure rutile titanium dioxide nanosheets electrochemically synthesized", Desalin. Water Treat., 194 (2020): 187-193, 2020.

[23] Ammar N.; Fahmy A.; Kanawy Ibrahim S.; Hamzawy E. M. A. and El-Khateeb M.; "Wollastonite ceramic/CuO nano-Composite For cadmium ions removal from waste water", Egypt. J. Chem.; 60 (5): 817-823, 2017.

[24] Ghibate R.; Senhaji O. and Taouil R.; "Kinetic and thermodynamic approaches on Rhodamine B adsorption onto pomegranate peel", Case Stud. Chem. Environ. Eng., 3: 100078, 2021.

[25] Safri A.; Fletcher A. J.; Abdel-Halim E.; Ismail M. A. and Hashem A.; "Calligonum crinitum as a novel sorbent for sorption of Pb (II) from aqueous solutions: thermodynamics, kinetics, and isotherms", J. Polym. Environ., 29 (5): 1505-1515, 2021.

[26] Lima E. C.; Gomes A. A. and Tran H. N.; "Comparison of the nonlinear and linear forms of the van't Hoff equation for calculation of adsorption thermodynamic parameters (Δ S° andΔ H°)", J. Mol. Liq., 311: 113315, 2020.

[27] Wu W.; Lu C.; Yuan M.; Tian Y. and Zhou H.; "Acidification of potassium bismuthate for enhanced visible-light photocatalytic degradation ability: an effective strategy for regulating the abilities of adsorption, oxidation, and photocatalysis", Appl. Surf. Sci.; 544: 148873, 2021.

[28] Zulfiqar M.; Chowdhury S.; Samsudin M. F. R.; Siyal A. A.; Omar A. A.; Ahmad T. and Sufian S.; "Effect of organic solvents on the growth of TiO_2 nanotubes: An insight into photocatalytic degradation and adsorption studies", Journal of Water Process Engineering, 37, 101491, 2020.

[29] Darwish A. A. A.; Rashad M. and Al-Aoh H. A.; "Methyl Lemon adsorption comparison on nanoparticles: Isotherm, kinetics, and thermodynamic studies", Dye. Pigment., 160: 563-571, 2019.

[30] Wang F.; "Adsorption of Anionic Dye on Graphene Nanosheets Doped with Ag Nanoparticles: Kinetics and Thermodynamic Study", Russ. J. Phys. Chem. A., 93 (7): 1357-1364, 2019.

[31] Regazzoni A. E.; "Adsorption kinetics at solid/aqueous solution interfaces: on the boundaries of the pseudo-second order rate equation", Colloids Surfaces A Physicochem. Eng. Asp., 585: 124093, 2020.